Targeting two distinct epitopes on human CD73 with a bispecific antibody improves anticancer activity

Odd L Gammelgaard [1], Mikkel G Terp [1], Christian Renn,[2] Aran F Labrijn,[3] Oliver Hamaker,[1] Aaraby Y Nielsen,[1] Henriette Vever,[1] Soren WK Hansen,[1] Morten F Gjerstorff,[1,4] Christa E Müller,[2] Paul WHI Parren,[1,5] Henrik J Ditzel [1,4]

¹Department of Cancer and Inflammation Research, Institute of Molecular Medicine, University of Southern Denmark, Odense, Denmark
²PharmaCenter Bonn, Pharmaceutical Sciences Bonn (PSB), Pharmaceutical Institute, Pharmaceutical & Medicinal Chemistry, University of Bonn, Bonn, Germany
³Genmab BV, Utrecht, The Netherlands
⁴Department of Oncology, Odense University Hospital, Odense, Denmark
⁵Department of Immunology, Leiden University Medical Center, Leiden, The Netherlands

Correspondence to
Dr Henrik J Ditzel;
hditzel@health.sdu.dk

ABSTRACT

Background Immunosuppressive extracellular adenosine is generated by the enzymatic activity of CD73. In preclinical models, antibodies (Abs) targeting different epitopes on CD73 exert anticancer activity through distinct mechanisms such as inhibition of enzymatic activity, engagement of Fc receptors, and spatial redistribution of CD73.

Methods Using controlled Fab arm exchange, we generated biparatopic bispecific antibodies (bsAbs) from parental anti-CD73 Abs with distinct anticancer activities. The resulting anticancer activity was evaluated using in vitro and in vivo models.

Results We demonstrate that different anticancer activities can be combined in a biparatopic bsAb. Remarkably, the bsAb significantly improved the enzyme inhibitory activity compared with the parental Abs, which led to neutralization of adenosine-mediated T-cell suppression as demonstrated by proliferation and interferon gamma (IFN-γ) production and prolonged survival of tumor-bearing mice. Additionally, the bsAb caused more efficient internalization of cell surface CD73 and stimulated potent Fc-mediated engagement of human immune effector cells in vitro and in vivo.

Conclusions Our data collectively demonstrate that complementary anticancer mechanisms of action of distinct anti-CD73 Abs can be combined and enhanced in a biparatopic bsAb. The multiple mechanisms of action and superior activity compared with the monospecific parental Abs make the bsAb a promising candidate for therapeutic targeting of CD73 in cancer. This concept may greatly improve future Ab design.

WHAT IS ALREADY KNOWN ON THIS TOPIC
⇒ Targeting non-overlapping epitopes on CD73 leads to distinct anticancer activity.

WHAT THIS STUDY ADDS
⇒ We demonstrate that desirable anticancer activities can be combined by application of bispecific antibodies.

HOW THIS STUDY MIGHT AFFECT RESEARCH, PRACTICE OR POLICY
⇒ The anticancer activity of antibodies can be improved by bispecific targeting. This may greatly affect future development of this very important class of cancer drugs.

BACKGROUND

Adenosine-mediated immune suppression is a major hurdle for reinstating functional cancer immunity.[1 2] The major source of extracellular adenosine originates from hydrolysis of released ATP. Specifically, CD39 converts ATP to AMP followed by CD73-mediated dephosphorylation. Mice genetically deficient of CD73 or the adenosine receptor $A_{2A}R$ are protected against tumor challenge.[3–5] Additionally, inhibition of adenosine-mediated immune suppression is additive to other modes of immunotherapy, including blockade of programmed cell-death 1 (PD-1) and cytotoxic T-lymphocyte associated protein 4 (CTLA-4),[6] either alone or in combination,[7] and adoptive cell therapy,[4 8] which has positioned CD73 as a promising target for next-generation immune-checkpoint blockers,[9] and paved the way for clinical evaluation of several anti-human CD73 antibodies (Abs) including MEDI9447 (MedImmune), CPI-006 (Corvus) and BMS-986179 (Bristol Myers Squibb).

Preclinical evaluation of the effect of CD73 inhibition has mainly been assessed by gene silencing,[10 11] by application of the small molecule inhibitor adenosine 5′-α,β-(methylene) diphosphate (APCP)[4 11–14] or the rat anti-mouse CD73 Ab TY23,[4–6 10 12–15] all of which have consistently demonstrated favorable anticancer immune-mediated responses. It is noteworthy that APCP[11] and TY23[10] provide more modest responses compared with gene silencing. Interestingly, while APCP effectively inhibits the enzymatic activity of CD73, the therapeutic activity of TY23 relies greatly

on the capacity to engage Fc receptors,[12] thus enhanced activity may be accomplished by designing Abs that can both effectively limit enzymatic activity and stimulate Fc receptors.

We, and others, have previously demonstrated that targeting different CD73 epitopes results in distinct biologic responses, including enzymatic inhibition and anti-metastatic activity.[16–19] Moreover, it was recently shown that biparatopic targeting of CD73 in some cases increased enzymatic inhibition by limiting spatial flexibility.[20] Thus, to maximize antitumor activity, we designed a bispecific Ab (bsAb) composed of Fab arms derived from an enzymatic inhibitory and an anti-metastatic parental Ab, respectively. This strategy led to greatly improved enzymatic inhibitory activity, which resulted in restoration of T-cell functionality and powerful engagement of anti-metastatic activity.

MATERIALS AND METHODS
Generation of bsAbs
bsAbs were generated through controlled Fab arm exchange (cFAE), as described previously.[21 22] In short, equimolar amounts of relevant human IgG1-(L234F-L235E-D265A-)F405L and IgG1-(L234F-L235E-D265A-)K409R or murine IgG2a-(L234A-L235A-)F405L-R411T and IgG2a-(L234A-L235A-)T370K-K409R Abs were mixed and incubated with 2-mercaptoethylamine (2-MEA; Sigma) at a final concentration of 1 mg/mL per antibody. The final concentration of 2-MEA was 75 mM. The mixtures were typically incubated for 5 hours at 31°C. To remove 2-MEA, the mixtures were buffer-exchanged against phosphate buffered saline (PBS) using PD-10 desalting columns (5 kDa molecular weight cut-off; GE Healthcare) or dialysis using Slide-A-Lyzer cassettes (10 kDa molecular weight cut-off; Pierce). Samples were stored overnight at 4°C to allow for reoxidation of the disulfide bonds. The efficacy of cFAE was assessed by hydrophobic interaction chromatography, as previously described.[23]

Lentiviral transduction
A sequence encoding a chimeric CD73 molecule comprising amino acid number 27-549 of human CD73 flanked by 1-28 and 551-579 murine CD73 was inserted into the pLenti6.2-ccdB-3xFLAG-V5 plasmid using the EcoRV and SacII restriction sites. pLenti6.2-ccdB-3xFLAG-V5 was a gift from Susan Lindquist & Mikko Taipale (Addgene plasmid # 87071; http://n2t.net/addgene:87071; RRID:Addgene_87071). The CD73 expression plasmid was prepared as lentivirus by Lentifectin (Abmgood)-mediated co-transfection with pMD2.G, pRSV-Rev, pMDL g/p RRE packaging plasmids (kindly provided by the Trone Lab through Addgene) into HEK293T cells. Virus was harvested from the supernatant after 3 days, filtered, precipitated with polyethylene glycol (PEG) and resuspended in PBS. Cells, 5×10⁴, were supplemented with lentivirus and 5 mg/mL polybren overnight and 72 hours

after infection stably transduced cells were sorted based on binding by the bsAb AD2×1E9.

Enzymatic activity
Enzymatic activity was determined as previously reported.[24 25] Briefly, cells, membrane fractions or recombinant soluble human CD73 expressed in Sf9 cells were preincubated with serially diluted Ab solutions in reaction buffer (25 mM Tris, 2 mM $MgCl_2$, 1 mM $CaCl_2$, 140 mM NaCl, pH 7.4). Cells were subsequently incubated in the presence of radiolabeled AMP ([³H] adenosine-5′-monophosphate, 5 µM, 20 mCi/mM) for 30 min at 37°C. The reaction was stopped by the addition of ice-cold phosphate buffer (100 mM NaH_2PO_4, pH 7.4) (1:1 v/v), and unreacted radiolabeled AMP was precipitated by the addition of x5 reaction volume lanthanum chloride dissolved in buffer (100 mM $LaCl_3$×7 H_2O, 100 mM NaOAc, pH 4.0), fivefold volume of the test solution, followed by 1 hour of incubation on ice. Samples were filtered through GF/B glass fiber filters, which were washed twice with approximately 3 mL of buffer. The eluent was collected, transferred to scintillation vials, and scintillation cocktail ULTIMA Gold XR was added. Radioactive [³H]adenosine formed by the enzymatic reaction was quantified by scintillation counting using a Tricarb 2900 TR, Packard/PerkinElmer. Enzymatic activity was calculated relative to untreated cells or membrane fractions, respectively. The enzymatic activity of CT26. CL25-hCD73 was assessed by the Malachite green phosphate detection kit (R&D Systems, DY996) according to the manufacturer's instructions.

Human interferon gamma (IFNγ) measurement
IFNγ secretion from T cells cultured with CD3/CD28 beads for 4 days was measured using the Human IFNγ uncoated ELISA kit (ThermoFisher, 88-7316-88) according to the manufacturer's instructions. In short, 96-well Nunc Maxisorp plates were coated with an anti-human IFNγ capture Ab. Wells were subsequently washed and blocked followed by 2-hour incubation (room temperature, shaking) with the samples. Wells were washed and captured IFNγ was detected by a second biotin-labeled anti-human IFNγ Ab. Following detection, wells were washed and incubated with streptavidin-labeled horseradish peroxidase. Following binding and washing, the substrate solution was added, the color reaction was followed by visual inspection and stopped by addition of stop solution. The plate was read using a Paradigm Detection platform (Beckman Coulter) and the difference in wavelength (450–570 nm) was calculated.

Cell trace proliferation
Negatively selected human T cells (5×10⁶) were labeled with CellTrace CSFE Cell Proliferation Kit (Invitrogen, C34554) according to the manufacturer's instructions. Labeled T cells (4×10⁴) were seeded in a sterile round-bottomed 96-well plate and serially diluted Abs were subsequently added. The cell Ab mixture was incubated

1 hour at 37°C to allow Ab binding. AMP was added to the cell suspension (200 µM final concentration) and incubated 30 min at 37°C. T cells were activated as described above and incubated 4 days at 37°C. Following incubation, cells were washed once in wash buffer (PBS supplemented with 2 mM EDTA, 2% heat-inactivated fetale bovine serum (FBS)) and stained with APC-H7 labeled mouse anti-human CD4 (BD Bioscience, 641398) and Brilliant Violet 421 labeled mouse anti-human CD8 (BD Bioscience, 740093). Following staining, cells were washed three times in wash buffer and analyzed by flow cytometry.

In vivo experiments

Eight to twelve-week-old female NOG (NOD.Cg-^{PrkdcSCID}Il-2^{rgtm1Sug}/JicTac, Taconic) were injected intravenously with 2×10^7 human PBMCs or PBMCs depleted of monocytes or T cells. Three days later, 5×10^5 MDA-MB-231-Luc2+ cancer cells preincubated with Abs for 30 min at 37°C were injected intravenously. One mouse from each group were challenged at a time to minimize confounders. Relative quantification of metastasis development was performed weekly using whole-body bioluminescent imaging (IVIS Spectrum; Caliper Life Science). Mice were injected with D-luciferin (150 mg/kg body weight) and then anesthetized with isoflurane gas. Images were acquired starting 10 min after luciferin injection. Regions of interest (ROIs) were drawn around the lungs to quantify metastases. The photon emission transmitted from the ROIs was quantified in photons/s/cm^2/sr using Caliper Life Science Living image. Alternatively, metastasis was quantified by immunohistochemistry (IHC) as detailed in the online supplemental materials and methods.

For adoptive transfer experiments, female Balb/C (BALB/cAnNTac, Taconic) mice were injected subcutaneously with 7×10^5 CT26.CL25 or CT26.CL25-hCD73 cells. Cancer development and rejection was followed by caliper measurement. Following cancer rejection, splenocytes were adoptively transferred to female NOG mice carrying 1-day-old CT26.CL25-hCD73 tumors. Tumor volume was calculated LxW^2/2. For tumor development and survival analysis, animals were considered dead when tumors reached a volume of 50 mm^3 or length of 1.2 cm, respectively. All animal experiments were performed at the animal core facility at the University of Southern Denmark. Mice were housed with ad libitum food and water. The light/dark cycle was 12 hours light/dark, with lights turned on from 06:00 to 18:00. Housing temperature was 21°C±1°C and relative humidity 40%–60%. Sample size was guided by previous experience and preliminary data. No animals were excluded from analysis. No randomization was performed as treatment was given before tumor size could be reliably determined. Investigators performing the experiments were not blinded. Mice were acclimatized for 2 weeks before initiation of experiments.

Statistical analysis

A two-tailed t-test, analysis of variance (ANOVA), Mann-Whitney or Log-rank (Mantel Cox) test was employed for in vitro and in vivo studies (indicated in the figure legends). For statistical analysis, GraphPad Prism V.8 (GraphPad Software) were used. P values<0.05 were considered statistically significant.

For further details regarding the materials and methods, please refer to the online supplemental information.

RESULTS

Targeting CD73 with a biparatopic bsAb stabilizes epitope recognition and increases Ab deposition

To study the potential benefit of combining distinct anti-cancer activities by biparatopic targeting of CD73, bsAbs were generated through controlled Fab arm exchange.[21 23] bsAbs were generated comprised of one Fab arm from each of the parental anti-human CD73 Abs AD2 and 1E9 (AD2×1E9), as well as functionally monovalent (AD2xb12 and 1E9xb12) control bsAbs, using b12 as irrelevant (non-binding) target arm.[26] The anti-human/mouse CD73 Ab MEDI9447 (Oleclumab),[27] which is undergoing clinical assessment, was included as a benchmark control Ab. In accordance with previous reports,[17] AD2 and 1E9 Abs did not compete for binding to CD73 as assessed by flow cytometry. As expected, both parental Abs competed with the bsAb AD2×1E9, indicating that the bsAb was able to interact with the epitopes of both parental Abs (figure 1A). Interestingly, the 1E9 Ab increased binding of the AD2 Ab in a cooperative-like manner, whereas binding by the 1E9 Ab was independent of the binding of the AD2 Ab (figure 1B,C). MEDI9447 competed with both AD2, 1E9 and the bsAb.

ATP and ADP, which are often found at relatively high concentrations in tumors, are well-described competitive inhibitors of CD73.[28] Mechanistically, they block the substrate binding site and keep the binding pocket in a closed conformation,[29] which could potentially sequester epitopes and thereby compromise Ab binding. We therefore examined whether binding was affected by the presence of the stable ADP-analog APCP. Indeed, the epitope recognized by 1E9 (both the parental and the monovalent control), but not that of AD2, was sensitive for modulation by APCP, as binding to it was significantly reduced in the presence of APCP (figure 1D, p<0.05). In contrast, binding by the bsAb AD2×1E9 was insensitive to APCP, suggesting that binding of the AD2 Fab arm stabilizes the epitope recognized by the 1E9 Fab. Taken together, these data demonstrate that the epitopes recognized by the AD2 and 1E9 Abs are non-overlapping and binding to one epitope favors binding to the other (figure 1E).

Next, we applied flow cytometry to compare each Ab in terms of apparent affinity and saturation level using the two cancer cell lines: MDA-MB-231 and A375. The loss of bivalency for both the AD2 and 1E9 Abs decreased their apparent affinities, indicating that both Abs can bind bivalently, although the effect was greater for AD2 (~10-fold decrease) compared with 1E9 (~2-fold decrease) (figure 1F and online supplemental figure 1A). Most importantly, the bsAb AD2×1E9 displayed higher
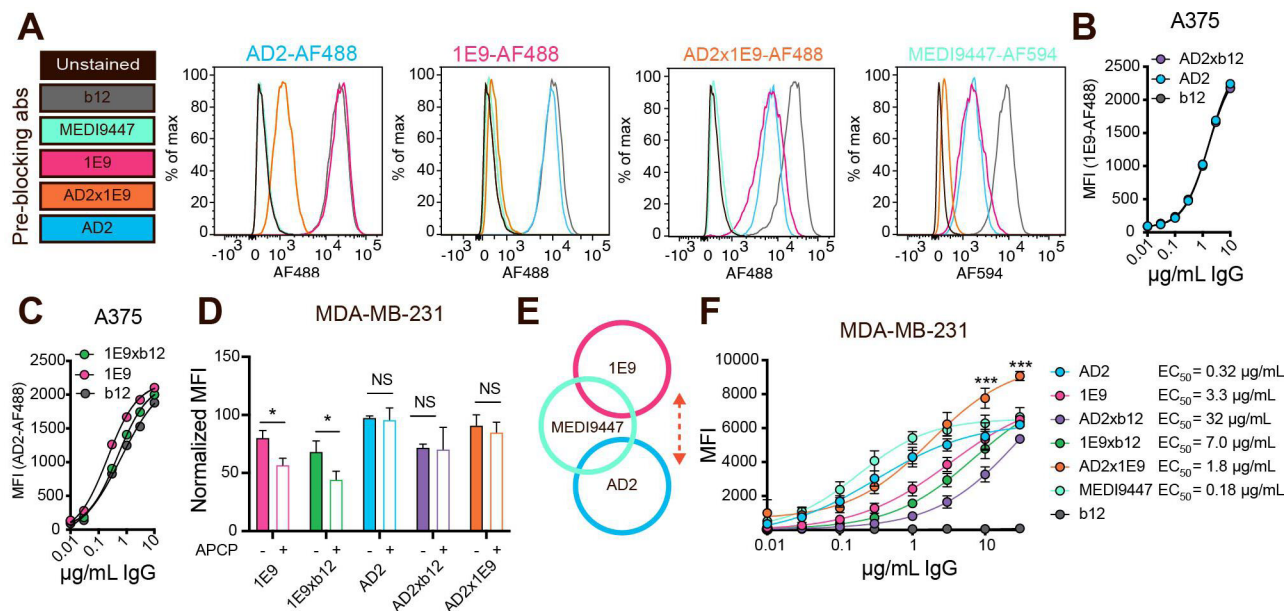
Figure 1 bsAb AD2×1E9 binds simultaneously with both Fab arms, is resistant to APCP-mediated epitope sequestration and exhibits increased Ab deposition. (A) Competition of fluorescently labeled Abs (AD2-AF488, 1E9-AF488, MEDI9447-AF594, bsAb AD2×1E9-AF488, 5 µg/mL) with preincubated non-labeled Abs (indicated to the left, 10 µg/mL) and analyzed by flow cytometry. Peaks shifted to the left indicate blocking of the labeled Ab. Panel (A) is representative of three independent experiments. (B, C) Increased binding by the AD2-AF488 in the presence of 1E9 and bsAb 1E9xb12 was observed, whereas binding of 1E9-AF488 was not affected by the presence of AD2 or bsAb AD2xb12, as determined by flow cytometry analysis. (D) Ab binding in the presence or absence of APCP as determined by flow cytometry analysis. Epitope recognition by anti-CD73 Abs was detected by addition of a secondary fluorescent-labeled Ab. Mean±SEM from three independent experiments is shown. Statistical difference was determined using paired t-tests. (E) Schematic representation of the epitope interactions. (F) Flow cytometry analysis of Ab binding to MDA-MB-231 cells using a similar setup as in panel (D). Mean±SEM from three independent experiments is shown. Statistical difference was determined by Student's t-test (D) or two-way ANOVA (F) method followed by Bonferoni's multiple comparison testing. *0.05>p≥0.01; **0.01>p≥0.001; ***0.001>p. Abs, antibodies; ANOVA, analysis of variance; bsAbs, bispecific antibodies; APCP, adenosine 5′-α,β-(methylene)diphosphate; NS non-significant.

apparent affinity compared with the functionally monovalent Abs (and intermediate to the apparent affinities of the parental bivalent clones), confirming simultaneous binding to both epitopes. As expected AD2, 1E9 and MEDI9447 displayed comparable saturation plateaus, which was significantly lower than that of bsAb AD2×1E9 (figure 1F, p<0.001). These results demonstrate that the bsAb AD2×1E9 binds both epitopes and increases the maximum Ab deposition level on the cancer cells.

The bsAb AD2x1E9 stimulate Fc-dependent anticancer activity in vitro and in vivo

We previously reported that AD2 (mouse IgG1), but not 1E9 (mouse IgG3), displayed anticancer activity in xenografted CB17 SCID mice by a mechanism involving clustering and internalization.[16] To further dissect this mechanism of action, we initially examined whether the Abs with human Fc regions stimulated clustering and internalization. As expected, AD2, but not 1E9 or MEDI9447, stimulated clustering and internalization of CD73 (figure 2A and online supplemental figures 2 and 3). The behavior of AD2 was completely recapitulated by the bsAb AD2×1E9. To investigate whether this anticancer activity was cancer cell intrinsic (eg, binding-dependent) or extrinsic (eg, Fc-dependent), we challenged NOG

mice (which have limited Fc receptor activity) with MDA-MB-231 cells pretreated with Fc-silenced Abs, and found that none of the Abs exerted anticancer activity (online supplemental figure 4), suggesting an extrinsic mechanism of action. Using human peripheral blood mononuclear cells (PBMCs), we therefore studied the capacity of the Abs to stimulate Fc-mediated killing. We discovered an unexpectedly slow, but highly effective, kill mechanism that displayed dose-dependent relationships with respect to both number of effector cells and Ab concentration (online supplemental figures 5A,B). Interestingly, AD2 and bsAb AD2×1E9 displayed significantly higher efficacy compared with 1E9 and MEDI9447 (figure 2B, p<0.001). A similar pattern was observed using MDA-MB-468 cells (online supplemental figure 5C). The cancer cell killing was not affected by the addition of AMP, suggesting that the mechanism was independent of enzymatic inhibition (online supplemental figure 5D). In accordance with the in vivo experiments, the kill capacity was completely lost using Abs that were Fc-silenced, but was intact using (functionally) monovalent bsAbs, demonstrating that it was independent of cross-linking target and effector cells (online supplemental figure 5E,F). Despite the slow cancer cell killing, we reasoned that antibody-dependent
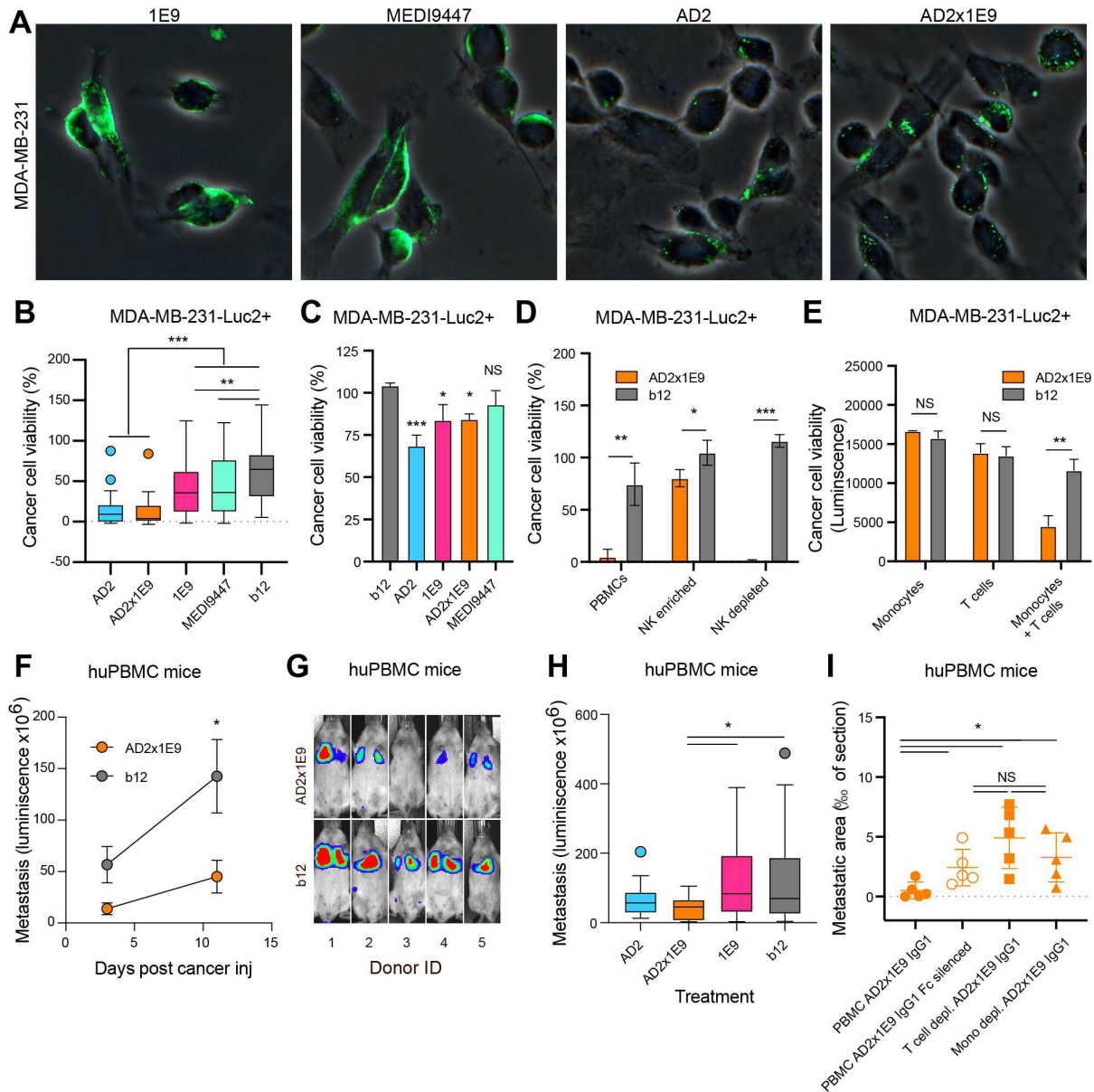
Figure 2 bsAb AD2×1E9 induces potent Fc-mediated cell death leading to anticancer activity. (A) Merged bright field and immunofluorescence images showing the surface pattern of CD73 on MDA-MB-231 cells following incubation with the indicated Abs, showing distinct clusters when incubated with AD2-derived Abs. (B) Cancer cell viability analysis (luminescence) following incubation with Abs (10 µg/mL) and human PBMCs at an effector-target (ET) ratio of 100:1 after 72 hours, demonstrating epitope-specific cancer cell killing. A Tukey box comprising data from peripheral blood mononuclear cells (PBMCs) of 24 healthy donors is shown. Statistical difference was determined by ANOVA followed by Bonferoni's multiple comparison testing. (C) Similar setup as for (B) but using purified Natural killer (NK) cells instead of PBMCs at an ET ratio of 12.5:1. A representative of two experiments is shown. (D) Similar setup as for (B, C) but comparing PBMCs, NK cells and PBMCs depleted of NK cells. The added NK to cancer cell ratio is 14 for both PBMCs and NK cell-enriched fractions, and five for NK cell-depleted fractions. A representative of three independent experiments is shown. (E) Similar setup as for (B–D) but comparing the effect of enriched monocytes and T cells separately and in combination. Monocytes and T cells were added at an ET ratio of 10 and 50, respectively. A representative of four experiments is shown. Statistical difference in (D–E) was determined by Student's t-tests. (F) Female age-matched NOG mice were transplanted with human PBMCs (2×10^7) from healthy donors, two mice per donor, each assigned to an intravenous injection with MDA-MB-231-luc2+ cells (10^5) preincubated with either bsAb AD2×1E9 or b12 Ab (n=5). Mean±SEM is shown. Statistical difference was determined by two-way ANOVA followed by Bonferoni's multiple comparison testing. (G) Similar to (F) showing raw in vivo bioimaging data demonstrating reduced cancer growth across PBMC donor matched mice. (H) As in (F) with a total of 10 donors (AD2 (n=10), 1E9 (n=10) and bsAb AD2×1E9 (n=15) and b12(n=15)) with read-out after 11 days. A Tukey box plot is shown, showing similar activity ranks of the anti-CD73 Abs as in (B) and online supplemental figure 5C. Statistical difference was determined by Student's t-test. (I) Similar setup as for (H) but evaluating the effect of Fc interactions, T cells and monocytes, respectively. Quantification is based on immunohistochemistry as described in the Materials and methods section. Statistical difference was determined by the Mann-Whitney test. *$0.05 > p \geq 0.01$; **$0.01 > p \geq 0.001$; ***$0.001 > p$. Abs, antibodies; ANOVA, analysis of variance; bsAbs, bispecific antibodies;; NS non-significant.
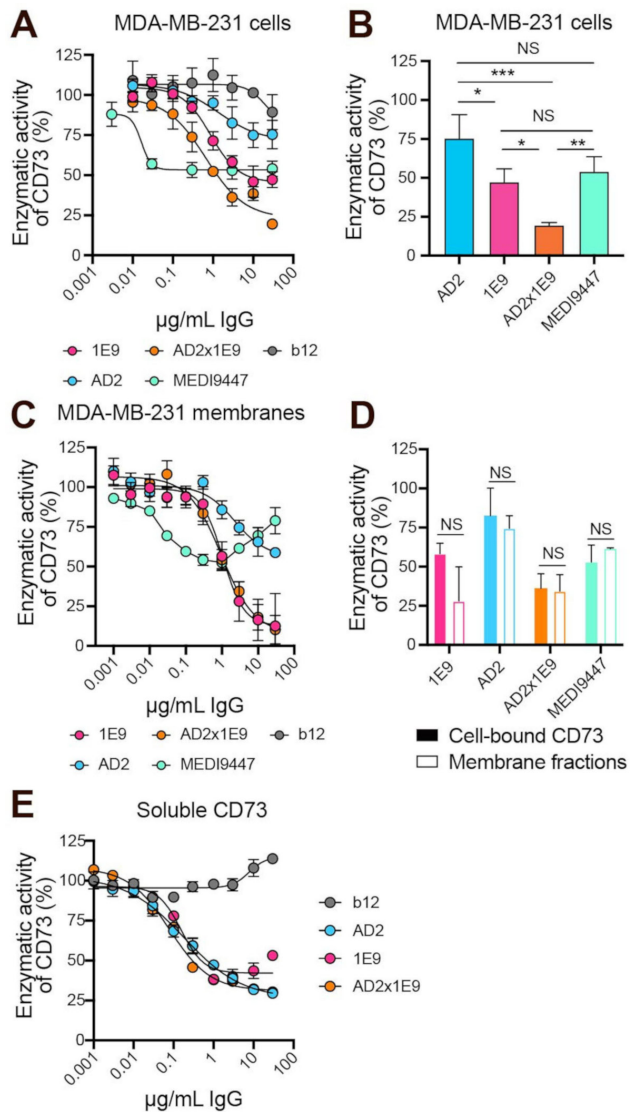
Figure 3 bsAb AD2×1E9 displays enhanced potency and efficacy in terms of inhibiting the enzymatic activity of CD73. (A) Enzymatic activity of CD73 on intact cells (MDA-MB-231) on incubation with serially diluted Ab solutions as measured by radiometry. Means±SEM from three to four independent experiments are shown. (B) Comparison of the enzymatic inhibition in panel (A) at 30 µg/mL. Mean±SD is shown. Statistical difference was determined by one-way ANOVA method followed by Sidak's multiple comparison testing. (C) Enzymatic activity of CD73 using membrane preparations from MDA-MB-231 cells on incubation with serially diluted Ab solutions as measured by radiometry. Mean±SEM from three to four independent experiments is shown. (D) Comparison of the enzymatic activity shown in panels (A) and (C) at concentrations that induced the largest effect, demonstrating similar activity of CD73 using intact cells and purified membranes. Mean±SD is shown. (E) Comparison of the enzymatic inhibition of recombinant soluble human CD73 on incubation with serially diluted Ab as measured by radiometry. Means±SEM from two independent experiments are shown. Statistical difference was determined by two-way ANOVA method followed by Sidak's multiple comparison testing. *0.05>p≥0.01; **0.01>p≥0.001; ***0.001>p. Abs, antibodies; ANOVA, analysis of variance; bsAb, bispecific antibodies; NS non-significant.

cellular cytotoxicity (ADCC) was the most likely mechanism of action. While natural killer cell mediated ADCC could be detected (figure 2C,D, p<0.05), the effect was very modest compared with that observed using PBMCs, and there was no difference between the efficacy when using either AD2, 1E9 or the AD2×1E9 bsAb, suggesting a NK-independent mechanism of action. Furthermore, NK depletion did not compromise the cancer cell killing in vitro (figure 2D, p<0.001). In addition to NK cells, PBMCs contain a substantial fraction of monocytes that may also express Fc receptors. To our surprise, monocytes did not exert any activity on their own but, on addition of T cells (that also did not exert activity on their own), the cancer cell killing mechanism was re-established (figure 2E, p<0.01).

To evaluate the effect of the observed epitope-specific Fc, T cell and monocyte-dependent cancer cell killing mechanism in vivo, we generated humanized immune system mice by transplantation of PBMC from five healthy donors (two mice per donor, each assigned to the bsAb AD2×1E9 and b12 treatment group, respectively) and monitored MDA-MB-231 cancer growth using in vivo bioimaging. As expected, we found that bsAb AD2×1E9 significantly inhibited cancer growth compared with control b12-treated mice (figure 2F,G, p<0.05). Importantly, mice reconstituted with PBMCs from all five donors benefitted from the bsAb therapy, although to variable extents (figure 2G). The growth inhibitory effect was confirmed using IHC of lungs at endpoint (online supplemental figure 5G). To directly compare the epitope dependence, we repeated the analysis using another five donors and compared the effect of bsAb AD2×1E9 to both AD2 and 1E9. In line with the in vitro assays, AD2×1E9 bsAb and AD2 displayed comparable activity, which were higher than that of the 1E9 Ab (figure 2H, p<0.05). Finally, to directly assess whether the observed in vivo activity was Fc, T cell and monocyte dependent, we created another cohort of humanized mice by transfer of either complete PBMCs or PBMCs depleted of either T cells or monocytes. As expected, depletion of either T cells or monocytes, or using an Fc-silenced version of the AD2×1E9 bsAb, compromised the anticancer activity (figure 2I, p<0.05). Taken together, these data demonstrate that the bsAb confers anticancer activity by a Fc-mediated mechanism that correlates with the capacity to drive surface clustering of CD73 and is dependent on both human monocytes and T cells, and independent of the inhibition of the enzymatic activity of CD73.

Targeting by the bsAb AD2x1E9 improves enzymatic inhibition of CD73

Next, we investigated the inhibitory capacity of each Ab in a highly sensitive enzymatic activity assay using MDA-MB-231 cells exhibiting high CD73 expression by measuring Abs potency (IC50) and efficacy (maximum inhibitory capacity).[24] As shown in figure 3A, all CD73 Abs inhibited the enzymatic activity of CD73 on intact cells in a concentration-dependent manner, but with highly

variable potency (tabulated in online supplemental table 1). Although the MEDI9447 Ab displayed approximately 50-fold higher potency compared with the 1E9 Ab (IC50 of 1.7×10^{-2} and 8.7×10^{-1} µg/mL, respectively), their efficacy was comparable under saturated concentrations, with approximately 50% residual enzymatic activity. The AD2, AD2xb12, and 1E9xb12 Abs all displayed both low efficacy and potency (figure 3A and online supplemental figure 6A). Importantly, the bsAb AD2×1E9 demonstrated increased potency compared with either of the AD2 and 1E9 Abs alone and superior efficacy compared with the AD2, 1E9 and MEDI9447 Abs with only 20% residual enzymatic activity (figure 3A,B, p<0.05).

To distinguish between direct enzymatic blocking and sequestration by internalization, we repeated the analysis using isolated membranes from MDA-MB-231 cells (figure 3C and online supplemental figure 6B). In line with previous data regarding soluble CD73,[27] MEDI9447 exhibited a 'hook-effect' with the highest efficacy at an Ab concentration of 1µg/mL. Similar to cell-bound CD73, approximately 50% residual enzymatic activity was observed for the MEDI9447 Ab (figure 3A,C). The hook effect was not observed for either the AD2, 1E9 or the bsAb AD2×1E9, which inhibited the enzymatic activity in a concentration-dependent manner. It is noteworthy that the efficacies of AD2, 1E9 and bsAb AD2×1E9 were comparable to those observed at cell-bound CD73, indicating that none of the Abs was dependent on internalizing CD73 for inhibiting its activity (figure 3D). Finally, we assessed the capacity of the Abs to inhibit the enzymatic activity of soluble human CD73. All anti-CD73 Abs displayed comparable and concentration-dependent enzymatic inhibition (figure 3E and online supplemental figure 6C). Taken together, these data demonstrate that the bsAb AD2×1E9 inhibit the enzymatic activity of cell-bound, membrane-bound and soluble CD73, and that it displays superior efficacy in terms of inhibiting the enzymatic activity of cell-bound CD73 compared with AD2, 1E9 and MEDI9447.

The bsAb AD2x1E9 protects T cells from adenosine-mediated suppression

Next, we investigated whether the different efficacies would be reflected in their capacities to protect T cells against adenosine-mediated suppression of cytokine production, activation, and proliferation. To that end, we stimulated human T cells using anti-CD3/anti-CD28 beads with and without AMP in the presence of the Ab panel (figure 4A). In line with its improved inhibitory activity, bsAb AD2×1E9 was significantly more effective at retaining IFNγ secretion compared with AD2, 1E9 and MEDI9447 (figure 4B, p<0.001). We then investigated whether T-cell proliferation could be preserved. None of the Abs induced T-cell activation (figure 4C, top row) or interfered with T-cell activation (figure 4C, middle row) on their own. As expected, activation and proliferation of T cells incubated with the control Ab b12 was largely compromised by AMP (figure 4C, left column).

Remarkably, the bsAb AD2×1E9, but not MEDI9447, 1E9 or AD2, completely protected the T cells as colony formation was retained (figure 4C). Similar results were obtained when blood from patients with cancer was used (online supplemental figure 7). To investigate this in a more quantitative manner, we labeled human T cells with carboxyfluorescein succinimidyl ester (CSFE) and assessed proliferation by flow cytometry. As depicted in figure 4D–F, the results were similar to those obtained by light microscopy. The rescuing effect was observed for both CD4 and CD8 T cells (figure 4D–F). Indeed, most T cells were found not to proliferate when incubated with MEDI9447, 1E9 or AD2, whereas the majority of those treated with the bsAb AD2×1E9 had undergone five divisions or more (figure 4D–F). As expected, the capacity to alleviate adenosine-mediated T-cell suppression was lost in a concentration-dependent manner (figure 4G), which correlated with the Abs' capacity to saturate CD73 binding (figure 1A) and enzymatic inhibition (figure 3A). Taken together, these data clearly demonstrate a benefit of targeting human CD73 with the bsAb AD2×1E9 to protect T-cell functionality.

bsAb AD2×1E9 therapy inhibits tumor growth

Neither the 1E9 nor the AD2 Ab bind mouse CD73, complicating evaluation of potential in vivo benefits relating to T cells.[16] Since Fc-related activities were studied in figure 2, we designed a model in which the enzymatic activity of cancer-derived human CD73 could be studied in the presence of murine T cells. To this end, we created a mouse tumor cell line expressing human CD73. This was accomplished by generation of a chimeric CD73 gene construct in which the human CD73 gene was flanked by the mouse leader sequence and mouse GPI-signal sequence (figure 5A), which was delivered to target cells using lentiviral transduction. We chose the CT26.CL25 model, as it is highly immunogenic and does not express murine CD73 in vitro (figure 5B). Expression and Ab recognition of the chimeric CD73 protein was confirmed by flow cytometry (figure 5C). Importantly, the enzymatic activity could both be inhibited (figure 5D) and internalized (figure 5E), resembling the effect observed when targeting human CD73 (figure 3) and as previously shown.[16] On transplantation of these cells, both syngeneic Balb/c and NOG mice developed CT26.CL25-hCD73 tumors, which were subsequently rejected in Balb/c, but not NOG mice. Furthermore, mice that rejected the tumor did not develop tumors on transplantation of a second dose of tumor cells, strongly indicating an immune-mediated mechanism. Human CD73 is most likely the responsible antigen, as the parental CT26.CL25 was not rejected in Balb/c mice (online supplemental figure 8). To establish a window in which cancer-reactive lymphocytes could be affected by anti-human CD73 Ab therapy, we transplanted CT26.CL25-hCD73 cells into Balb/c mice, allowed cancer rejection to occur, and adoptively transferred splenocytes to CT26.CL25-hCD73 challenged NOG mice. These mice were randomized into
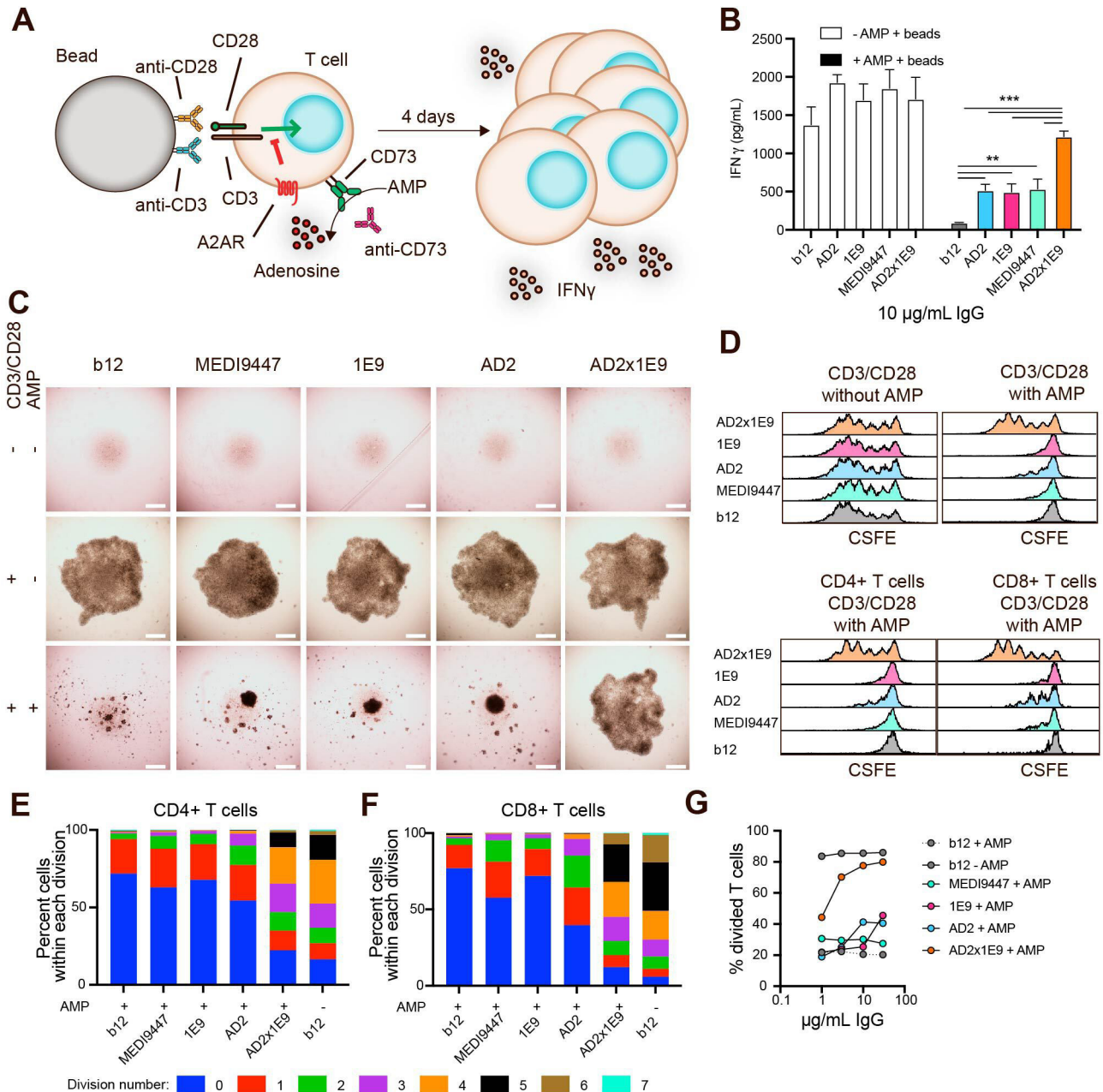
Figure 4 The bsAb AD2×1E9 effectively protects T cell functionality. (A) Schematic depiction of the experimental setup. (B) ELISA analysis of secreted IFNγ from T-cell supernatants on 4 days incubation with CD3/CD28 beads (at a cell-to-bead ratio of 1:1), AMP (200 µM), and the indicated Abs (10 µg/mL). A representative of three independent experiments, performed in triplicate is shown. Statistical difference was determined by one-way ANOVA followed by Bonferoni's multiple comparison testing. (C) Bright field images showing the extent of expansion of purified T cells exposed as in panel (B). The images show no/low proliferation rate (top row), high proliferation rate (middle row), and various proliferation rates (bottom row). Scale bar 500 µm. (D) Flow cytometry analysis showing division-induced dilution of carboxyfluorescein succinimidyl ester (CSFE)-labeled T cells on exposures as in panel (B). Both total T cells (in the presence and absence of AMP), and gated CD4-positive T cells and CD8-positive T cells (in the presence of AMP) are shown. (E, F) Bar chart showing the frequency of CSFE-labeled CD4-positive and CD8-positive T cells, respectively, within 0–7 divisions on exposures as in panels (B). (G) Flow cytometry analysis showing the frequency of divided CSFE-labeled T cells at various concentrations of Ab on activation and inhibition as in panel (A). (C–G) Representative of three independent experiments. **0.01>p≥0.001; ***0.001>p. Abs, antibodies; bsAbs, bispecific antibodies; ANOVA, analysis of variance; IFNγ, interferon gamma.

groups receiving various murine IgG2a Fc-silenced Abs (to specifically study the effect of targeting the enzymatic activity) (figure 5F). As expected, and in accordance with figures 3 and 4, bsAb AD2×1E9 therapy significantly prolonged survival (median survival of 14 days) compared

with any of the parental therapies (median survival of 7 days), which did not prolong survival compared with control therapy (figure 5G, p<0.05). To evaluate how long the beneficial effect could be maintained, we repeated the experiment and allowed tumors to reach maximum
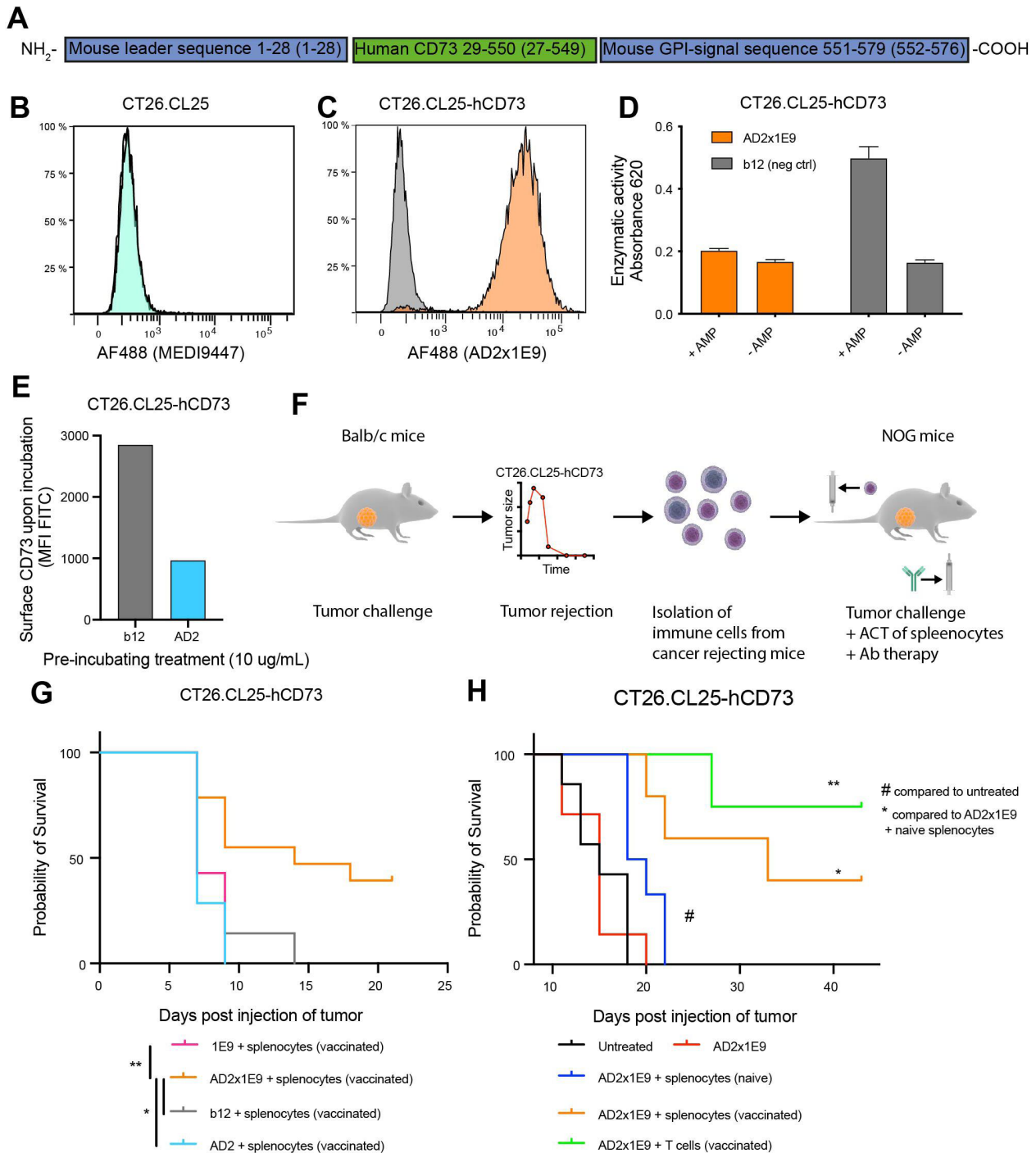
Figure 5 Targeting CD73 with the bsAb AD2×1E9 inhibits tumor growth. (A) Schematic outline of the chimeric mouse/human CD73 construct. Numbers indicate amino acid residues. Numbers in parentheses indicate their location in syngeneic species. (B, C) Flow cytometry analysis demonstrating lack of surface mouse CD73 on CT26.CL25 cells (B) and expression of human CD73 on CT26.CL25-hCD73 cells (C). Representative of two independent experiments is shown. (D) Enzymatic activity of chimeric CD73 on incubation with 10 µg/mL Ab as measured by the Malachite green assay, illustrating inhibitory activity of the bsAb AD2×1E9. A representative of three independent experiments performed in triplicates is shown. (E) Flow cytometry analysis illustrating removal of surface CD73 by the AD2 Ab on 3-hour incubation. (F) Schematic illustration of the ACT experiment workflow. (G) Female NOG mice were injected subcutaneously with $7×10^5$ CT26.CL25-hCD73 cells. On day 1, mice were injected intravenously with PBS or $2×10^7$ splenocytes from female Balb/c CT26.CL25-hCD73 rejecting mice. On days 1 and 8, mice were treated with 200 µg Fc-silenced Ab or PBS intraperitoneally. Mean±SEM is shown. n=14 (AD2×1E9), n=7 (AD2), n=7 (1E9), n=7 (b12). (H) Mice were challenged as described in (G) and left untreated (n=7), treated with AD2×1E9 as monotherapy (n=7), or with AD2×1E9 in combination with either $2×10^7$ splenocytes from unvaccinated mice (n=6), $2×10^7$ splenocytes from vaccinated mice (n=6), or $5×10^6$ T cells from vaccinated mice (n=4). All bsAb constructs were Fc-silenced. Statistical difference in survival was determined by log-rank (Mantel-Cox) test. *p<0.05; **0.01>p≥0.001; ***p<0.001. Abs, antibodies; bsAbs, bispecific antibodies; ACT, adoptive cell transfer.

legal size. To demonstrate that the effect was due to the combined activity of the bsAb AD2×1E9 and tumor-reactive T cells, we compared groups receiving AD2×1E9 as monotherapy, AD2×1E9 in combination with splenocytes from naïve mice, or AD2×1E9 in combination with splenocytes or purified T cells from tumor-vaccinated mice. In accordance with online supplemental figure 4, Fc-silenced AD2×1E9 exerted no detectable benefit as monotherapy in NOG mice (figure 5H). The addition of naïve splenocytes conferred a transient benefit, although all mice eventually succumbed to their tumor challenge (figure 5H, p<0.05). In contrast, combining Fc-silenced AD2×1E9 with splenocytes or T cells from vaccinated mice provided a prominent survival benefit, with approximately 50% presenting with complete tumor rejection (figure 5H, p<0.01). Indeed, tumor mass from mice treated with splenocytes or T cells from vaccinated mice in combination with the bsAb AD2×1E9 were significantly smaller than controls at the end of the experiment (online supplemental figure S9). Taken together, these data demonstrate that targeting the enzymatic activity of CD73 with the bsAb AD2×1E9 greatly enhances the functional activity of tumor-reactive T cells in vivo.

DISCUSSION

Multiple preclinical studies have revealed a detrimental effect of adenosine on anticancer immunity and hence the potential of inhibiting this effect by anti-CD73 Abs. This has led to the development of several anti-CD73 Abs that are currently undergoing clinical assessment. CD73 has been shown to exert several distinct cancer-promoting functions, and simultaneous inhibition of these functions may increase the anticancer effect of CD73-targeted treatment. In the current study, we demonstrate that unique desirable anticancer activities of specific anti-human CD73 Ab clones can be combined and potentiated when binding arms are joint in a biparatopic bsAb. Targeting by the bsAb greatly enhanced (1) enzymatic inhibition, (2) surface removal of CD73, and (3) stimulation of Fc-engaging effector functions. These combined mechanisms of action translate into desirable anticancer activities both in vitro and in vivo.

At least three anti-CD73 Abs (MEDI9447, CPI-006, and BMS986179) are currently undergoing clinical assessment in phase I and II clinical trials (ClinicalTrial.gov identifier: NCT03267589, NCT03454451, NCT02754141). We demonstrated that bsAb AD2×1E9 more effectively inhibits the enzymatic activity of human CD73 compared with MEDI9447. In accordance with our data, others have recently described suboptimal in vitro activity of the MEDI9447 Ab in terms of inhibiting the enzymatic activity.[30] In that study, it was further shown that the novel-CD73 Ab IPH5301 was superior to MEDI9447 at inhibiting the enzymatic activity, but displayed comparable efficacy in rescuing T-cell proliferation from AMP-mediated suppression. In contrast, we found a markedly improved effect of bsAb AD2×1E9 compared

with MEDI9447 in terms of inhibiting the enzymatic activity, rescuing T-cell proliferation, and restoring cytokine production. Relatively little information has been reported regarding the CD73 targeting Abs CPI-006[31] and BMS986179.[32] CPI-006 was reported to completely block enzymatic activity of CD73 when analyzed by the Malachite green assay.[31] Although promising, the low sensitivity of such assays warrant caution in interpretation. Accordingly, in our hands, 1E9 displayed <5% residual activity using the Malachite green assay, but approximately 50% when measured by the radiometric assay. Furthermore, T-cell proliferation and IFNγ production was only partially restored by CPI-006, whereas bsAb AD2×1E9 completely restored both while displaying approximately 20% residual enzymatic activity. BMS986179 presumably induces near-complete internalization of CD73.[32] In our hands, a fraction of CD73 appeared to be refractory to internalization. Interestingly, a comparable fraction was reported to be resistant to phosphatidyl-specific phospholipase C-mediated GPI cleavage.[33–36] Whether the capacity to completely internalize CD73 is indeed a unique and distinctive characteristic of BMS986179, or whether this Ab targets the same epitope as AD2, warrant further investigations.

From a mechanistic point of view, CD73 undergoes extensive domain movements during binding of its substrate AMP followed by hydrolysis,[29] and enzymatic inhibitory Abs have been reported to limit such movements.[27 30] Considering the equal affinity, but dramatic increase in enzymatic inhibition of the bsAb compared with the parental Abs, it is unlikely that the bsAb functions as a competitive antagonist. Instead, we propose that the increased Ab deposition by bsAb AD2×1E9 further enforces spatial rigidity accounting for the increased enzymatic inhibition compared with the parental Abs. This provides a plausible explanation for the decreased binding sensitivity in the presence of the competitive antagonist, the nucleotide analog APCP. The proposed model of enforced rigidity as a consequence of biparatopic targeting immediately suggests that other flexible Ab targets may benefit from similar approaches.

CD73 expression is increased in several types of cancer compared with non-malignant tissue,[1] and Ab-mediated internalization represents an attractive mechanism for normalizing the level of overexpressed antigens.[37] Biparatopic targeting has been reported to decrease surface expression of several receptors, including epidermal growth factor receptor (EGFR), erythroblastic oncogene b (ErbB-2),[38] and mesenchymal-epithelial transition factor (MET).[39] In line with these reports, we found an increased internalization rate and prolonged reduction of CD73 surface expression when targeted by the bsAb AD2×1E9. Efficient internalization of CD73 not only precludes enzymatic activity but also potential non-enzymatic cancer-promoting activities.

Human CD73 has been reported to confer resistance toward TRAIL-induced apoptosis[40] and to mediate adhesion and migration along the metastatic niche component

Tenascin C in vitro.[41 42] Although the relevance of these interactions has not yet been determined in vivo, we envision that inhibition of such mechanisms may result in increased anticancer activity.

In addition to inhibiting the enzymatic activity and limiting CD73 surface expression, the cluster inducing Abs (ie, Abs containing an AD2-derived Fab arm) were particularly effective at stimulating PBMC-mediated cancer cell killing, which translated into metastasis control in mice humanized by injection of PBMCs. We hypothesize that the selectively enhanced activity of the cluster-inducing Abs occurs (at least in part) because of massive aggregation of Fc fragments, leading to maturation and activation of Fc receptor expressing effector cells. Indeed, aggregated Fc fragments are known to stimulate oligomerization of Fc receptors, which is required for proper signal transduction.[43] In accordance with our data, Fc receptor-mediated signaling in myeloid cells does not linearly depend on target expression, but is largely organized as an all or none response on reaching an activation threshold.[44] On activation, monocytes/macrophages likely phagocytose opsonized cancer cells but require T cell help to destroy phagocytosed content. Despite the ability to engage human effector cells, the ubiquitous expression of CD73 on non-cancerous tissue calls into question the safety of Fc-receptor engagement. Encouragingly, the rat-anti-mouse Ab TY23 (IgG2a) has been extensively studied in mice with no indication of toxicities.[4–6 10 12 13 15 45] Additionally, several CD73-targeting Abs recently demonstrated enhanced in vivo activity when targeting both the enzymatic activity and facilitating Fc receptor engagement.[12 13] Thus, to the extent to which murine models recapitulate human biology, targeting CD73 with Fc-engaging Abs appears to be safe and partly responsible for the antitumor activity.

Evaluating the in vivo antitumor efficacy of non-cross species immune-modulatory reactive Abs remains a major challenge in cancer research. To accomplish this, we designed an adoptive cell transfer model using murine cancer cells expressing a chimeric mouse/human CD73 construct. Since only cancer cells can express the chimeric CD73 construct, only cancer-derived adenosine can be inhibited in our model. Nevertheless, it remains well established that both tumor[10] and host cells[4 5 12 14 46 47] expressing CD73 contribute to immunosuppression. The host-derived contribution can be substantial, as evidenced by significant benefit of targeting CD73 with APCP in wild type mice, but not in CD73-/- mice.[4 47] Since the potential benefit of targeting host CD73 is omitted from our model, the observed benefit is likely to greatly underestimate the potential of the bsAb AD2×1E9.

Taken together, we conclude that the bsAb AD2×1E9 exerts effective blockade of enzymatic cancer-promoting functions of CD73, effectively sequestering CD73 from potential interaction partners through internalization, while potently stimulating Fc receptor engagement. The multiple mechanisms of action and high activity demonstrate that our approach bears promise for therapeutic intervention of CD73-mediated immune dampening in cancer.

ORCID iDs
Odd L Gammelgaard http://orcid.org/0000-0002-5911-7276
Mikkel G Terp http://orcid.org/0000-0002-4468-6900
Aran F Labrijn http://orcid.org/0000-0001-9239-8439
Aaraby Y Nielsen http://orcid.org/0000-0003-2199-2857
Soren WK Hansen http://orcid.org/0000-0002-8186-4630
Morten F Gjerstorff http://orcid.org/0000-0002-0845-1952
Christa E Müller http://orcid.org/0000-0002-0013-6624
Paul WHI Parren http://orcid.org/0000-0002-4365-3859
Henrik J Ditzel http://orcid.org/0000-0003-3927-5135

REFERENCES

1 Allard B, Allard D, Buisseret L, *et al*. The adenosine pathway in immuno-oncology. *Nat Rev Clin Oncol* 2020;17:611–29.
2 Vijayan D, Young A, Teng MWL, *et al*. Targeting immunosuppressive adenosine in cancer. *Nat Rev Cancer* 2017;17:709–24.
3 Ohta A, Gorelik E, Prasad SJ, *et al*. A2A adenosine receptor protects tumors from antitumor T cells. *Proc Natl Acad Sci U S A* 2006;103:13132–7.

4 Wang L, Fan J, Thompson LF, *et al*. CD73 has distinct roles in nonhematopoietic and hematopoietic cells to promote tumor growth in mice. *J Clin Invest* 2011;121:2371–82.

5 Stagg J, Beavis PA, Divisekera U, *et al*. CD73-deficient mice are resistant to carcinogenesis. *Cancer Res* 2012;72:2190–6.

6 Allard B, Pommey S, Smyth MJ, *et al*. Targeting CD73 enhances the antitumor activity of anti-PD-1 and anti-CTLA-4 mAbs. *Clin Cancer Res* 2013;19:5626–35.

7 Hatfield SM, Kjaergaard J, Lukashev D, *et al*. Immunological mechanisms of the antitumor effects of supplemental oxygenation. *Sci Transl Med* 2015;7:277ra30.

8 Beavis PA, Henderson MA, Giuffrida L, *et al*. Targeting the adenosine 2A receptor enhances chimeric antigen receptor T cell efficacy. *J Clin Invest* 2017;127:929–41.

9 Allard D, Allard B, Gaudreau P-O, *et al*. CD73-adenosine: a next-generation target in immuno-oncology. *Immunotherapy* 2016;8:145–63.

10 Stagg J, Divisekera U, McLaughlin N, *et al*. Anti-CD73 antibody therapy inhibits breast tumor growth and metastasis. *Proc Natl Acad Sci U S A* 2010;107:1547–52.

11 Jin D, Fan J, Wang L, *et al*. CD73 on tumor cells impairs antitumor T-cell responses: a novel mechanism of tumor-induced immune suppression. *Cancer Res* 2010;70:2245–55.

12 Young A, Ngiow SF, Barkauskas DS, *et al*. Co-inhibition of CD73 and A2AR adenosine signaling improves anti-tumor immune responses. *Cancer Cell* 2016;30:391–403.

13 Vijayan D, Barkauskas DS, Stannard K, *et al*. Selective activation of anti-CD73 mechanisms in control of primary tumors and metastases. *Oncoimmunology* 2017;6:e1312044.

14 Stagg J, Divisekera U, Duret H, *et al*. CD73-deficient mice have increased antitumor immunity and are resistant to experimental metastasis. *Cancer Res* 2011;71:2892–900.

15 Loi S, Pommey S, Haibe-Kains B, *et al*. CD73 promotes anthracycline resistance and poor prognosis in triple negative breast cancer. *Proc Natl Acad Sci U S A* 2013;110:11091–6.

16 Terp MG, Olesen KA, Arnspang EC, *et al*. Anti-human CD73 monoclonal antibody inhibits metastasis formation in human breast cancer by inducing clustering and internalization of CD73 expressed on the surface of cancer cells. *J Immunol* 2013;191:4165–73.

17 Thompson LF ABL, Franklin ML, Gutensohn W. CD73 workshop panel report. In: Schlossman LB SF, Gilks W, Harlan JM, eds. *Leukocyte typing*. Oxford University Press, 1995: 564–7.

18 Airas L, Niemelä J, Salmi M, *et al*. Differential regulation and function of CD73, a glycosyl-phosphatidylinositol-linked 70-kD adhesion molecule, on lymphocytes and endothelial cells. *J Cell Biol* 1997;136:421–31.

19 Airas L, Niemelä J, Jalkanen S. CD73 engagement promotes lymphocyte binding to endothelial cells via a lymphocyte function-associated antigen-1-dependent mechanism. *J Immunol* 2000;165:5411–7.

20 Stefano JE, Lord DM, Zhou Y, *et al*. A highly potent CD73 biparatopic antibody blocks organization of the enzyme active site through dual mechanisms. *J Biol Chem* 2020;295:18379–89.

21 Labrijn AF, Meesters JI, de Goeij BECG, *et al*. Efficient generation of stable bispecific IgG1 by controlled Fab-arm exchange. *Proc Natl Acad Sci U S A* 2013;110:5145–50.

22 Labrijn AF, Meesters JI, Bunce M, *et al*. Efficient generation of bispecific murine antibodies for pre-clinical investigations in syngeneic rodent models. *Sci Rep* 2017;7:2476.

23 Labrijn AF, Meesters JI, Priem P, *et al*. Controlled Fab-arm exchange for the generation of stable bispecific IgG1. *Nat Protoc* 2014;9:2450–63.

24 Freundlieb M, Zimmermann H, Müller CE. A new, sensitive ecto-5'-nucleotidase assay for compound screening. *Anal Biochem* 2014;446:53–8.

25 Bhattarai S, Pippel J, Scaletti E, *et al*. 2-Substituted α,β-methylene-ADP derivatives: potent competitive Ecto-5'-nucleotidase (CD73) inhibitors with variable binding modes. *J Med Chem* 2020;63:2941–57.

26 Roben P, Moore JP, Thali M, *et al*. Recognition properties of a panel of human recombinant Fab fragments to the CD4 binding site of gp120 that show differing abilities to neutralize human immunodeficiency virus type 1. *J Virol* 1994;68:4821–8.

27 Geoghegan JC, Diedrich G, Lu X, *et al*. Inhibition of CD73 AMP hydrolysis by a therapeutic antibody with a dual, non-competitive mechanism of action. *MAbs* 2016;8:454–67.

28 Zimmermann H. 5'-Nucleotidase: molecular structure and functional aspects. *Biochem J* 1992;285:345–65.

29 Knapp K, Zebisch M, Pippel J, *et al*. Crystal structure of the human ecto-5'-nucleotidase (CD73): insights into the regulation of purinergic signaling. *Structure* 2012;20:2161–73.

30 Perrot I, Michaud H-A, Giraudon-Paoli M, *et al*. Blocking antibodies targeting the CD39/CD73 immunosuppressive pathway Unleash immune responses in combination cancer therapies. *Cell Rep* 2019;27:2411–25.

31 Piccione EC H A, Mikesell G, Daine-Matsuoka B. Preclinical and initial phase I clinical characterization of CPI-006: an anti-CD73 monoclonal antibody with unique immunostimulatory activity. *Soc Immunother Cancer Abstract* 2018;353.

32 Barnhart BC, Sega E, Yamniuk A, Hatcher S, *et al*. Abstract 1476: a therapeutic antibody that inhibits CD73 activity by dual mechanisms. *Cancer Res* 2016;76:1476.

33 Dianzani U, Redoglia V, Bragardo M, *et al*. Co-stimulatory signal delivered by CD73 molecule to human CD45RAhiCD45ROlo (naive) CD8+ T lymphocytes. *J Immunol* 1993;151:3961–70.

34 Resta R, Thompson LF. T cell signalling through CD73. *Cell Signal* 1997;9:131–9.

35 Thomson LF, Ruedi JM, Glass A, *et al*. Production and characterization of monoclonal antibodies to the glycosyl phosphatidylinositol-anchored lymphocyte differentiation antigen ecto-5'-nucleotidase (CD73). *Tissue Antigens* 1990;35:9–19.

36 Thompson LF, Ruedi JM, Low MG. Purification of 5'-nucleotidase from human placenta after release from plasma membranes by phosphatidylinositol-specific phospholipase C. *Biochem Biophys Res Commun* 1987;145:118–25.

37 Prewett M, Rockwell P, Rockwell RF, *et al*. The biologic effects of C225, a chimeric monoclonal antibody to the EGFR, on human prostate carcinoma. *J Immunother Emphasis Tumor Immunol* 1996;19:419–27.

38 Ben-Kasus T, Schechter B, Lavi S, *et al*. Persistent elimination of ErbB-2/HER2-overexpressing tumors using combinations of monoclonal antibodies: relevance of receptor endocytosis. *Proc Natl Acad Sci U S A* 2009;106:3294–9.

39 Grandal MM, Havrylov S, Poulsen TT, *et al*. Simultaneous targeting of two distinct epitopes on MET effectively inhibits MET- and HGF-driven tumor growth by multiple mechanisms. *Mol Cancer Ther* 2017;16:2780–91.

40 Mikhailov A, Sokolovskaya A, Yegutkin GG, *et al*. CD73 participates in cellular multiresistance program and protects against TRAIL-induced apoptosis. *J Immunol* 2008;181:464–75.

41 Sadej R, Skladanowski AC. Dual, enzymatic and non-enzymatic, function of ecto-5'-nucleotidase (eN, CD73) in migration and invasion of A375 melanoma cells. *Acta Biochim Pol* 2012;59:647–52.

42 Oskarsson T, Acharyya S, Zhang XH-F, *et al*. Breast cancer cells produce tenascin C as a metastatic niche component to colonize the lungs. *Nat Med* 2011;17:867–74.

43 Goodridge HS, Underhill DM, Touret N. Mechanisms of Fc receptor and dectin-1 activation for phagocytosis. *Traffic* 2012;13:1062–71.

44 Zhang Y, Hoppe AD, Swanson JA. Coordination of Fc receptor signaling regulates cellular commitment to phagocytosis. *Proc Natl Acad Sci U S A* 2010;107:19332–7.

45 Forte G, Sorrentino R, Montinaro A, *et al*. Inhibition of CD73 improves B cell-mediated anti-tumor immunity in a mouse model of melanoma. *J Immunol* 2012;189:2226–33.

46 Koszałka P, Gołuńska M, Stanisławowski M, *et al*. CD73 on B16F10 melanoma cells in CD73-deficient mice promotes tumor growth, angiogenesis, neovascularization, macrophage infiltration and metastasis. *Int J Biochem Cell Biol* 2015;69:1–10.

47 Yegutkin GG, Marttila-Ichihara F, Karikoski M, *et al*. Altered purinergic signaling in CD73-deficient mice inhibits tumor progression. *Eur J Immunol* 2011;41:1231–41.